Online Supplemental Material: Image Acquisition and Data Analysis

Data Acquisition

All imaging experiments were performed on a 3T MRI system with a maximum gradient strength of 45 mT/m and a maximum single direction slew rate of 200 mT/m/ms (Tim Trio, Siemens, Erlangen, Germany), using a twice-refocused balanced spin-echo diffusion echo-planer imaging pulse sequence (1) with fat suppression. Each session included independent DSI and DKI acquisitions, with the DTI data being taken as a subset of the DKI acquisition. To quantify variability for each dMRI method, each volunteer was scanned during two separate sessions, resulting in a total of 6 complete DSI and DKI datasets. The dMRI protocols were optimized to maximize the SNR rather than minimize the acquisition times in order to facilitate the assessment of the accuracy of DKI and DTI fiber orientation estimates relative to those of DSI.

Acquisition parameters common to both DSI and DKI acquisitions were: voxel size = 2.7 × 2.7 × 2.7 mm^3, matrix = 82 × 82, number of slices = 45, bandwidth = 1356 Hz/Pixel, and a 32 channel head coil with an acceleration factor of 2 using generalized autocalibrating partially parallel acquisition (2) and adaptive combine coil mode (3). Additional parameters for the DSI acquisition were TR/TE = 8300/151 ms and a total of 515 diffusion encoding gradient directions over a Cartesian grid with a maximum b-value of 6000 s/mm^2, which was optimized for diffusion sensitivity and gradient performance (4), resulting in a total acquisition time of 71.7 minutes. For the DKI acquisitions, additional parameters were TR/TE = 6100/102 ms, 64 diffusion encoding gradient directions at b-values of 1000 s/mm^2 and 2000 s/mm^2 , and a total of 20 independent acquisitions without diffusion weighting (b0 images), resulting in a total acquisition time of 15.6 minutes. In both cases, TE was minimized to maximize SNR. DTI data were also analyzed using the 0 and 1000 s/mm^2 b-value images from the DKI dataset. During each session, an additional T1-weighted magnetization-prepared rapid gradient echo (MPRAGE) image with 1.0 × 1.0 × 1.0 mm^3 voxel dimensions was also acquired for anatomical reference. By assuming

Online Supplemental Material: Image Acquisition and Data Analysis

80% of the maximum gradient strength (45 mT/m), i.e. 36 mT/m, was used to achieve the minimum echo time δ and Δ can be estimated to be 32 ms and 74 ms for the DSI scan, and for 22.5 ms and 50 ms for the DKI scan, respectively.

DODF Reconstructions

Each scan for each subject was co-registered to the subject's initial DSI scan using a 12-parameter affine transformation with SPM12 (Wellcome Trust Center for Neuroimaging, London, UK). Following co-registration, spatial smoothing was applied to all diffusion weighted images to reduce the effects of signal noise using a Gaussian smoothing kernel of 1.25 times the voxel dimensions (5).

The intra-voxel DSI dODF was reconstructed using DSI Studio (dsi-studio.labsolver.org, Department of Psychology, Carnegie Mellon University) with a Hanning filter of width 17 applied to the q-space data. DKI-derived diffusion and kurtosis tensors were calculated using a constrained weighted linear least squares algorithm (5), and the DKI dODF was calculated using the closed form solution derived by Jensen et al. (6). The DTI-derived diffusion tensor was obtained by using weighted linear least squares (7). Following previous studies, the radial weighting power was set to $\alpha = 2$ for DSI (8,9) and $\alpha = 4$ for DKI (6,10,11). For visualization of DTI dODFs, the radial weighting power was set to $\alpha = 4$; however this has no effect on the DTI-derived orientation estimates (6,10). All orientations were corrected for rotations of the image volume that occurred during image acquisition and co-registration (12). The kurtosis dODF reconstruction was performed using the Diffusional Kurtosis Estimator Fiber Tractography Module (https://www.nitrc.org/projects/dke/), and the DTI dODF was reconstructed using in-house software.

Online Supplemental Material: Image Acquisition and Data Analysis

Data Analysis

Angular variability of the dODFs was calculated by the absolute voxel-wise angular difference for each reconstruction between the principal orientation (the orientation corresponding to the global maxima pair) from the first scan and the nearest orientation from the second scan. Angular errors in the DKI and DTI dODFs were calculated using the absolute angular differences between the principal orientation from the corresponding DSI scan and the nearest dODF maximum from the respective reconstruction. For angular difference measures, the nearest orientation in the second scan was chosen as opposed to the global maximum from the second scan as small fluctuations in dODF magnitudes in voxels with multiple orientation estimates could vary which orientation was identified as the global maximum resulting in artificially large angular differences (10). Angular error estimates include intrinsic variability in the reconstruction techniques and hence combine both random and systematic error. In addition, because absolute differences are employed, these measures are positively biased by noise and will consequently overestimate the true systematic differences.

To quantify angular variability and angular error, ROIs were defined for each subject. These include an inclusive WM ROI, which was defined as voxels with FA > 0.1; a conservative WM ROI, which was defined as voxels with FA > 0.3; a single fiber bundle ROI, which was defined as voxels within the inclusive WM ROI with the estimated number of fiber directions (NFD) equal to 1 in the DSI scan; a two crossing fibers ROI, which was defined as voxels within the inclusive WM ROI with NFD = 2 in the DSI scan; and a 3 or more crossing fibers ROI, which was defined as voxels within the inclusive WM ROI with NFD $\geq$ 3 in the DSI scan. To reduce CSF partial volume effects, voxels within each ROI with mean diffusivity > 1.5 $\mu m^2/ms$ were excluded from quantitative analyses (6,10). To help reduce the occurrence of spurious peaks in

the DSI reconstruction a quantitative anisotropy threshold of 0.1 was used to filter the DSI orientations (13).

To visualize group differences in the angular variability and angular error measures, parameter maps from each subject were normalized to the International Consortium for Brain Mapping WM template (14) using SPM12 with non-linear registration, and average, group-wise parameter maps were constructed.

Tractography

WM fiber tractography was performed with DSI Studio using the Euler method (15) with a step size of 1.35 mm, a minimum track length of 20 mm, and a maximum track length of 450 mm. For direct and qualitative comparison across the three techniques, a common WM tracking ROI was defined to include regions in the inclusive WM ROI with quantitative anisotropy > 0.1 in the DSI scan. The fiber tracking algorithm was seeded with 200,000 random seed points within the WM tracking ROI. WM fiber tracts were visualized using TrackVis (trackvis.org, Martinos Center for Biomedical Imaging, Massachusetts General Hospital).

References

1. Reese TG, Heid O, Weisskoff RM, Wedeen VJ. Reduction of eddy-current-induced distortion in diffusion MRI using a twice-refocused spin echo. Magn Reson Med. 2003;49:177-82.
2. Griswold MA, Jakob PM, Heidemann RM, Nittka M, Jellus V, Wang J, Kiefer B, Haase A.Generalized autocalibrating partially parallel acquisitions (GRAPPA). Magn Reson Med. 2002 Jun;47(6):1202-10.

Online Supplemental Material: Image Acquisition and Data Analysis

3. Walsh DO, Gmitro AF, Marcellin MW. Adaptive reconstruction of phased array MR imagery. Magn Reson Med 2000;43:682– 690.
4. Kuo LW, Chen JH, Wedeen VJ, Tseng WY. Optimization of diffusion spectrum imaging and q-ball imaging on clinical MRI system. Neuroimage. 2008;41:7-18.
5. Tabesh A, Jensen JH, Ardekani BA, Helpern JA. Estimation of tensors and tensor-derived measures in diffusional kurtosis imaging. Magn Reson Med. 2011;65:823-36.
6. Jensen JH, Helpern JA, Tabesh A. Leading non-Gaussian corrections for diffusion orientation distribution functions. NMR Biomed. 2014;27:202-11.
7. Basser PJ, Mattiello J, Le Bihan D. Estimation of the effective self-diffusion tensor from the NMR spin echo. J Magn Reson. 1994;103:247-54.
8. Wedeen VJ, Hagmann P, Tseng WY, Reese TG, Weisskoff RM. Mapping complex tissue architecture with diffusion spectrum magnetic resonance imaging. Magn Reson Med. 2005;54:1377-86.
9. Wedeen VJ, Wang RP, Schmahmann JD, Benner T, Tseng WY, Dai G, Pandya DN, Hagmann P, D'Arceuil H, de Crespigny AJ. Diffusion spectrum magnetic resonance imaging (DSI) tractography of crossing fibers. Neuroimage. 2008;41:1267-77.
10. Glenn GR, Helpern JA, Tabesh A, Jensen JH. Optimization of white matter fiber tractography with diffusional kurtosis imaging. NMR Biomed. [online, doi: 10.1002/nbm.3374].
11. Neto Henriques R, Correia MM, Nunes RG, Ferreira HA. Exploring the 3D geometry of the diffusion kurtosis tensor-Impact on the development of robust tractography procedures and novel biomarkers. Neuroimage. 2015;111:85-99.
12. Leemans A, Jones DK. The B-matrix must be rotated when correcting for subject motion in DTI data. Magn Reson Med. 2009;61:1336-49.

13. Yeh FC, Verstynen TD, Wang Y, Fernández-Miranda JC, Tseng WY. Deterministic diffusion fiber tracking improved by quantitative anisotropy. PLoS One. 2013;8:e80713.
14. Mori S, Wakana S, Nagae-Poetscher LM, van Zijl PC. MRI Atlas of Human White Matter. Elsevier: Amsterdam; 2005.
15. Basser PJ, Pajevic S, Pierpaoli C, Duda J, Aldroubi A. In vivo fiber tractography using DT-MRI data. Magn Reson Med. 2000;44:625-32.

Online Supplemental Material: Figures

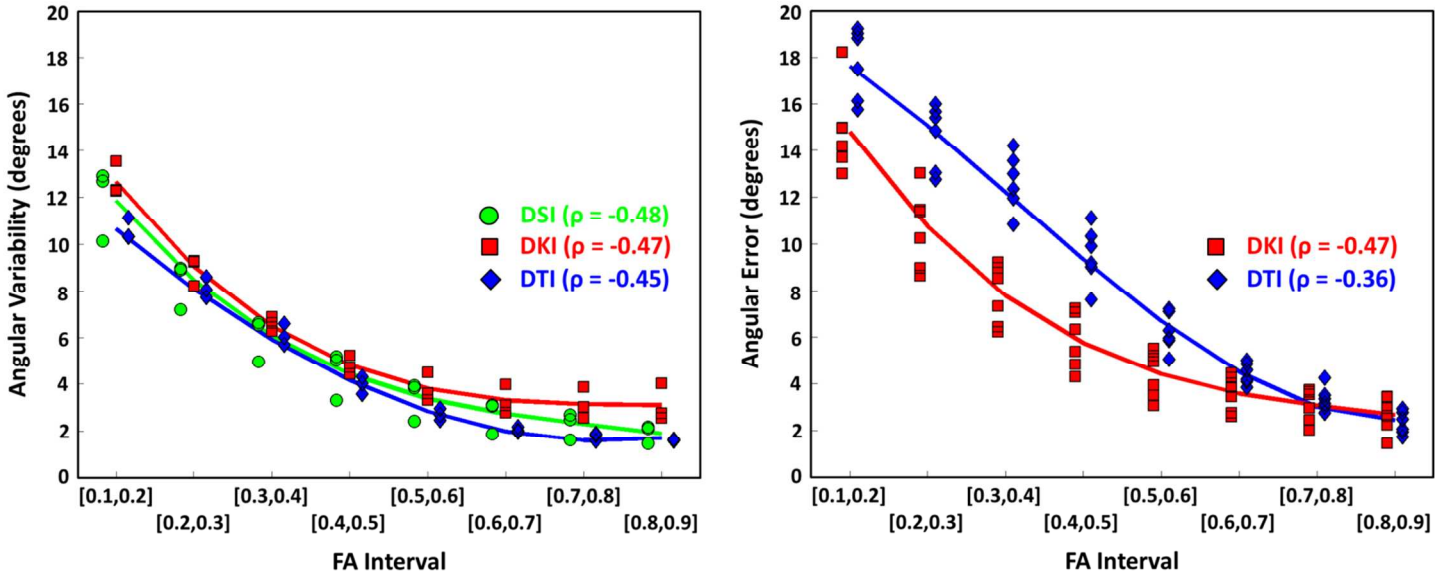

Supplemental Figure 1. The performance of dODF-derived orientation estimates depends on FA with angular variability and angular error decreasing with increasing FA. Data points for each group are averaged over the indicated interval and are separated in the horizontal direction within each interval for legibility. Spearman's rank correlation coefficient for the voxel-wise performance measure relative to FA is indicated by ρ.

Online Supplemental Material: Figures

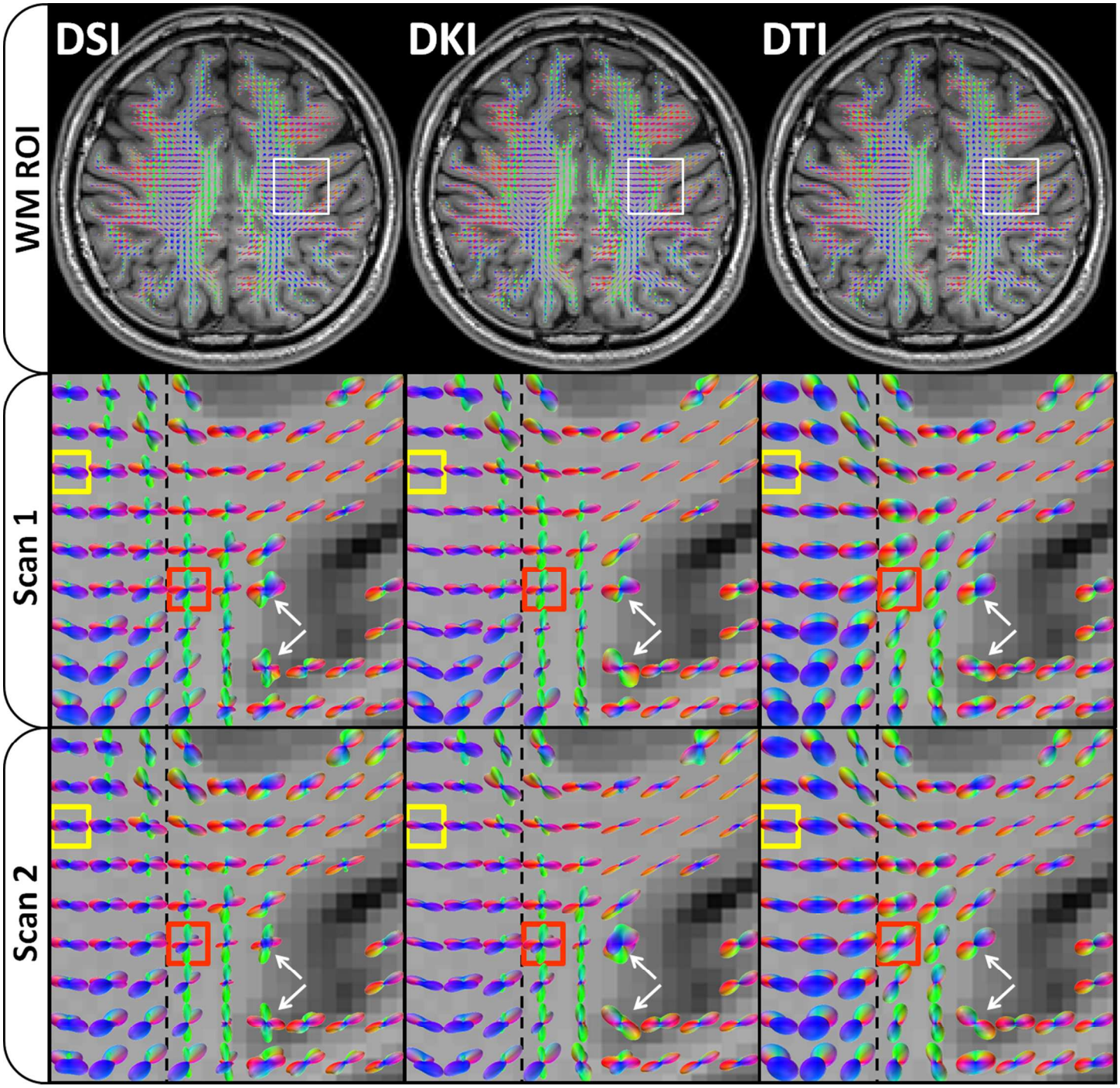

Supplemental Figure 2. For each reconstruction, dODFs within the inclusive WM ROI are overlaid on the MPRAGE image for anatomical reference. The dODF reconstructions are qualitatively consistent between repeated scans, but DTI cannot detect crossing fibers (red box), which may increase angular error relative to DSI. DSI is more sensitive than DKI at detecting crossing fibers (yellow box). The inclusive WM ROI may include partial volume effects (white arrow), which may increase variability and error in orientation estimates.